NACA

RESEARCH MEMORANDUM

THE FREQUENCY CONTENT OF THE CONTROL INPUT AND AIRPLANE

RESPONSE OBTAINED DURING SERVICE OPERATIONS

OF FIGHTER AIRPLANES

By John P. Mayer and Harold A. Hamer

Langley Aeronautical Laboratory
Langley Field, Va.

UNCLASSIFIED

NATIONAL ADVISORY COMMITTEE
FOR AERONAUTICS
WASHINGTON
July 12, 1957

CONFIDENTIAL

NATIONAL ADVISORY COMMITTEE FOR AERONAUTICS

RESEARCH MEMORANDUM

THE FREQUENCY CONTENT OF THE CONTROL INPUT AND AIRPLANE

RESPONSE OBTAINED DURING SERVICE OPERATIONS

OF FIGHTER AIRPLANES

By John P. Mayer and Harold A. Hamer

SUMMARY

The frequency content of the control input and resulting airplane motions is presented as power spectral densities for one operational flight of a fighter airplane. The frequency content, which is described by the shape of the spectrum, may be useful in providing inputs for the design of power control systems. For normal load factor, the results presented for the operational flight considered are in general agreement with the results of more complete data on three fighter airplanes.

The frequency content for the three control positions was similar and the frequency content for the three angular velocities was also similar when normalized by dividing by the mean-square value.

INTRODUCTION

In the design of power control systems and automatic pilots, it would be advantageous if the airplane motions and control motions necessary for the operation of the airplane in performing its missions were known in a form suitable to be used as inputs for the systems. One form which would be useful is the frequency content of time histories of the maneuvers performed in operational missions. The National Advisory Committee for Aeronautics, with the cooperation of the Air Force and the Bureau of Aeronautics, Department of the Navy, has been making an investigation of the manner in which military airplanes are used in service-training operations and some of the results are presented in references 1, 2, and 3. As a byproduct of these investigations some information has been obtained on the frequency content of the control inputs and airplane motions obtained by using power-spectral-analysis methods. The frequency content which is described by the shape of the spectra may be useful in providing inputs for the design of automatic or power control systems.

CONFIDENTIAL

The power spectral densities of the control inputs and resulting airplane motions obtained in one operational training flight of the Republic F-84G airplane are presented in this paper. Power spectral densities of angular velocity are also presented for an operational flight made by another jet fighter airplane (Republic F-84F). In addition, power spectral densities of the normal load factor obtained from several operational training flights are presented for the F-84F and the North American F-86A airplanes.

SYMBOLS

f	frequency, cps
$F(2\pi i f)$	Fourier transform, $\displaystyle\int_0^\infty f(t)e^{-2\pi i f t}dt$
K	constant used in filter equation
m	total number of observations
n	normal load factor
Δn	incremental normal load factor, $(n-1)$
$\left\|\dfrac{\Delta n}{\Delta \delta_E}\right\|$	amplitude ratio (see eq. (5) of ref. 2)
p	rolling velocity, radians/sec
q	pitching velocity, radians/sec
r	yawing velocity, radians/sec
$\dot{p}$	rolling acceleration, radians/sec^2
$\dot{q}$	pitching acceleration, radians/sec^2
$\dot{r}$	yawing acceleration, radians/sec^2
t	time, sec
T	time interval, sec
$\left\|T(f)\right\|$	amplitude ratio of frequency response
Δt	time reading interval, sec

y   quantity, Δn, p, q, δ_E, and so forth

$\overline{y}$ mean value of y

y'' filtered value of y; at time t,
$$y''_t = {}^K y_{(t-\Delta t)} - {}^2 y_{(t)} + {}^K y_{(t+\Delta t)}$$

$y(t), f(t)$ time history of quantity

α angle of attack, deg

β angle of sideslip, deg

δ control deflection, deg

δ_E elevator angle, deg

δ_A aileron angle, deg

δ_R rudder angle, deg

$\dot{\delta}$ control deflection rate, deg/sec

$\dot{\delta}_E$ elevator deflection rate, deg/sec

$\dot{\delta}_A$ aileron deflection rate, deg/sec

$\dot{\delta}_R$ rudder deflection rate, deg/sec

σ root-mean-square value of y, $\sigma^2 = \dfrac{\sum (y - \overline{y})^2}{m} = \displaystyle\int_0^\infty \Phi(f)_y \, df$

$\Phi(f)_y$ power spectral density of y,

$$\Phi(f)_y = \lim_{T \to \infty} \frac{1}{T} \left| \int_{-T}^T \left[y(t) - \overline{y(t)} \right] e^{-2\pi i f t} \, dt \right|^2 \quad \text{(ref. 4)}$$

AIRPLANE, INSTRUMENTATION, AND TESTS

The airplane for which most of the data are presented was a service model of the Republic F-84G airplane. In addition, some load-factor and angular-velocity data are presented for the North American F-86A and the Republic F-84F airplanes. The F-84G has unswept wings and the F-86A and F-84F have swept wings. The F-84G had a conventional elevator control

system but hydraulic boost was provided for the aileron control. The F-86A was equipped with a hydraulically boosted elevator and aileron and had an adjustable stabilizer. The F-84F had an all-movable stabilator and all controls were hydraulically boosted. The F-84F was equipped with spoilers in addition to ailerons.

Except for the addition of sideslip and angle-of-attack booms, neither the external appearance nor the weight and balance of the airplanes was altered by the addition of the instrumentation. Three-view drawings of each airplane are presented in figure 1.

Standard NACA instruments were used to record airspeed, altitude, control position, the three linear and three angular accelerations, the three angular velocities, angle of attack, and angle of sideslip. Details of the instrumentation are given in reference 1.

The flights were performed by service pilots during regular squadron operational training. The F-84G was flown with tip tanks and the F-86A was flown without external tanks. The F-84F was flown with and without wing tanks. Data were recorded during those flights in which the mission was scheduled to include a large number of maneuvers and were recorded continuously throughout these flights. Although not requested, most of the maneuvers were performed in relatively smooth air; no attempt was made to specify the type or severity of maneuvers.

The flight of the F-84G airplane selected for presentation in this paper contained most of the tactical maneuvers that are within the capabilities of the airplane and, in addition, was considered the flight most representative of all the flights obtained with this airplane. The flight contained acrobatics, dive bombing, and ground gunnery and was about 46 minutes in length. The percentages of time spent in various altitude, airspeed, and Mach number ranges for this flight are shown in figure 2. (It might be noted that the airspeed was obtained by using the airplane service system and was not corrected for position error.)

For the F-86A airplane the average altitude was 14,100 feet, the average Mach number was 0.58, and the average indicated airspeed was 298 knots. The average values for the F-84F airplane were: altitude, 10,500 feet; Mach number, 0.62; and indicated airspeed, 343 knots.

METHODS OF ANALYSIS

The frequency content of a time history of a quantity $f(t)$ is ordinarily given as the amplitude of the Fourier transform:

$$F(2\pi i f) = \int_0^\infty f(t) e^{-2\pi i f t} dt \tag{1}$$

The power spectrum given by the equation

$$\Phi(f) = \lim_{T \to \infty} \frac{1}{T} \left| \int_{-T}^{T} f(t) e^{-2\pi i f t} dt \right|^2 \tag{2}$$

is a convenient way of presenting the frequency content for long time histories of a quantity. Essentially, the power spectral densities may be considered proportional to the amplitude squared of the frequency content ordinarily obtained from the Fourier transform. In addition, the power spectrum of the output or response is directly related to the power spectrum of the input through the transfer function by the equation

$$\Phi(f)_{input} = |T(f)|^2 \Phi(f)_{output} \tag{3}$$

The methods described in reference 4 were used in determining the power spectral densities. All of the records were read at 0.5-second intervals, and 40 estimates of the power at frequencies up to 1 cycle per second were obtained by using digital computing methods. In addition to the spectra computed from records read at 0.5-second intervals, spectra were also computed from the data taken at 2-second intervals to provide more detail on estimates of power at the lower frequencies. Also, for pitching and yawing accelerations, spectra were computed from records read at 0.2-second intervals to provide additional information at frequencies up to 2.5 cycles per second. The power spectra presented are the spectra with the mean subtracted $\Phi(f)_{(y-\bar{y})}$.

In order to improve the accuracy of the computed spectra, the spectra was first obtained of an altered (filtered) time history of the quantity given by the equation

$$y''_t = Ky_{(t-\Delta t)} - 2y_{(t)} + Ky_{(t+\Delta t)} \quad (K < 1) \tag{4}$$

This is essentially a high-pass filter which retains some information at zero frequency. This particular expression was used because it was

found to make the spectra relatively constant over the frequency range when the appropriate value of K was used. The values of K used varied from 0.97 to 0.70 for the spectra presented in this paper. The spectrum of y" was then converted to the spectrum of y by the equation

$$\Phi(f)_y = \frac{\Phi(f)_{y''}}{\left[2K \cos(2\pi f \Delta t) - 2\right]^2} \tag{5}$$

The spectra of the derivative $\dot{y}$ of the measured quantities were obtained from the following equation:

$$\Phi(f)_{\dot{y}} = (2\pi f)^2 \Phi(f)_y \tag{6}$$

RESULTS AND DISCUSSION

The power spectra define the range of frequencies within which the control system must be able to operate. For example, if the frequency content of control positions necessary for an airplane to perform its missions was negligible above frequencies of 2 cycles per second the control system would have to operate only in the range up to 2 cycles per second. The frequency content of the control input and airplane response is shown in figures 3 to 10 in the form of power spectral densities plotted against frequency.

Inasmuch as the frequency characteristics of the control systems of the test airplanes could influence the frequency content obtained for the control motions and airplane responses, these characteristics were examined. It was found that the control systems for all of the airplanes tested were capable of responding considerably beyond the frequencies obtained in this paper (i.e., $f > 2.5$ cps); therefore, the frequency characteristics of the control systems would have little effect on the results obtained.

Normal Load Factor

In figure 3 the power spectral densities of incremental normal load factor are shown for flight 2 of the F-84G airplane. Also shown are the spectra for flights 1 and 2 combined of the F-84G (see ref. 3), spectra for three flights of the F-86A airplane and 50 flights of the F-84F airplane. (In each case the power spectral densities have been divided by

the mean square.) The power spectral densities are relatively constant at the lowest frequencies and then decrease approximately with $f^{-2.5}$ at the highest frequencies. The spectrum from flight 2 of the F-84G airplane is similar to the combined spectra for flights 1 and 2. The spectra for the F-86A and F-84F airplanes are also similar.

Control Positions

In figure 4 the power spectrum of elevator angle is shown for flight 2 of the F-84G airplane. Results are shown for three sections of the flight; each section consisted of about 15 minutes of flight. The power spectral densities for each of the three parts appear to be very similar and decrease approximately with $f^{-2.5}$.

A comparison of the spectra of the elevator angle, aileron angle, and rudder angle for flight 2 of the F-84G are shown in figure 5. The spectra have been normalized by dividing by the mean square in each case.

Although there are some differences, the spectra for the three control positions are roughly the same and decrease approximately with $f^{-2.5}$ at the higher frequencies.

The derived spectra of control rates are shown in figure 6. The spectra increase with frequency at frequencies up to about 0.10 cycle per second and then remain relatively constant up to 1 cycle per second.

Angle of Attack and Sideslip

The normalized spectra for angle of attack and sideslip are shown in figure 7. The spectra decrease approximately with f^{-3} at the higher frequencies. The power spectral densities of the sideslip angle are higher than those of the angle of attack at frequencies above 0.1 cycle per second. It is believed that this is representative only of this particular flight and would not necessarily be representative of a larger sample. In this particular flight there were a number of large sideslip variations at frequencies above 0.1 cycle per second which caused the differences in the spectra. Because the data are plotted on a log scale the differences appear to be magnified.

Angular Motions

In figure 8 are shown the normalized spectra of pitching, rolling, and yawing angular velocities for the F-84G airplane. The normalized

spectra for the three angular velocities are approximately equal and decrease with f^{-2} at the higher frequencies.

In order to supplement the information given in figure 3 where the load-factor spectra of the F-84G are compared with those of other fighter airplanes, angular-velocity spectra were determined from data obtained in one flight with the F-84F airplane. Normalized spectra of pitching, rolling, and yawing angular velocities for a 50-minute flight of the F-84F airplane are given in figure 9. Also shown in the figure is a curve representing the angular-velocity spectra of the F-84G which was obtained by fairing a line through the data in figure 8. It is apparent in figure 9 that the normalized spectral densities of the three angular velocities for the F-84F airplane are not equal over the frequency range such as those shown in figure 8 for the F-84G airplane. The largest difference is in the rolling-velocity spectrum which is considerably higher than the pitching- and yawing-velocity spectra at the higher frequencies. The noticeable peak in the yawing-velocity spectrum at a frequency of about 0.6 cycle per second is caused by the directional oscillations which are characteristic of many fighter airplanes when flying at high speeds or in rough air. This peak may also be noted in the yawing-velocity spectrum of the F-84G although it is not as pronounced. (See fig. 8.) The leveling-off of the pitching-velocity spectrum at high frequency may be due to the longitudinal short-period motion of the airplane. Although the data in figure 9 represent relatively small samples, it is indicated that angular-velocity spectra are similar for the two airplanes. It is possible that if larger samples of data were used the F-84F angular-velocity spectra would more closely resemble each other and those of the F-84G airplane.

The spectra of the angular accelerations for the F-84G airplane are shown in figure 10. In addition to the spectra derived by using equation (6), the records of yawing and pitching acceleration were read at 0.2-second intervals and the spectra obtained from these records are included to extend the frequency range up to 2.5 cycles per second. The results for all these angular accelerations are about the same. The power spectral densities increase with frequency at frequencies up to about 0.05 cycle per second, remain relatively constant between 0.05 and 0.7 cycle per second, and then decrease rapidly at higher frequencies (approximately with f^{-3}).

In figure 10 the measured spectra agree with the spectra derived from equation (6). This is shown more clearly in figure 11 where for the F-84G airplane the spectrum of yawing acceleration obtained from the measured values is compared with the spectrum derived from the yawing-velocity spectrum for a section of flight 2. The spectrum obtained from the measured values is shown for the records read at 0.5-second intervals at frequencies up to 1 cycle per second. The agreement is very good except at the lowest frequencies where the measured spectral densities

do not increase with frequency as do the derived spectral densities. The derived values are believed to be better in this region because the statistical reliability is low for the first two points of the measured spectra.

Alternate Representation of Spectra

The spectra for the quantities in figures 3 to 10 indicate that the power spectral densities decrease rapidly at high frequencies. Although power spectral densities are normally plotted as log-log plots as in figures 3 to 10, the frequency content is more graphically illustrated if $f\Phi(f)$ is plotted against log f. For example, the root-mean-square value is

$$\sigma^2 = \int_0^\infty \Phi(f)\,df \tag{7}$$

which may also be expressed as

$$\sigma^2 = \int_0^\infty f\Phi(f)\,d\log f \tag{8}$$

In figure 12, a typical example is given where $f\Phi(f)/\sigma^2$ is plotted against log f. In this figure the portion of the root mean square contributed in various frequency ranges is directly proportional to the area under the curve. Two curves are shown in figure 12. The solid curve was obtained from an average of the control-position data shown in figure 5 and the dashed line was obtained from the angular-acceleration data shown in figure 10. The solid curve, however, is typical not only of the control positions but also of the load factor and the angular velocities. The dashed curve is typical of the angular accelerations and the control rates.

From figure 12 it may be shown that about 95 percent of the root-mean-square values of the control positions, load factor, and angular velocities is contained in frequencies less than 0.2 cycle per second. Also, about 90 percent of the area falls between frequencies of 0.002 cycle per second and 0.2 cycle per second. The area was concentrated at approximately 0.02 to 0.03 cycle per second.

For the angular accelerations and control rates it can be seen that the area has shifted to higher frequencies and is concentrated at approximately 0.6 to 0.7 cycle per second. In this case about 95 percent of

███████

the root-mean-square value was contained at frequencies less than
1.5 cycles per second and about 90 percent of the area falls between
frequencies of 0.08 and 1.5 cycles per second.

Derivation of Elevator-Angle Spectrum

One of the uses of the power spectrum is that, if the spectrum of
the output is known, the spectrum of the input is related directly through
the transfer function. In figure 13 the spectrum of the measured elevator
angle is compared with the spectrum of the elevator angle derived from
the load-factor spectrum (eq. (3)). The transfer function was calculated
for an average value of Mach number, altitude, weight, and center-of-
gravity location. The stability derivatives used in the transfer function
were obtained from available wind-tunnel tests. The agreement between
the actual and derived values shown in figure 13 appears to be good con-
sidering that average values of the parameters and wind-tunnel results
were used in calculating the transfer function.

CONCLUDING REMARKS

The frequency content of the control input and resulting airplane
motions has been presented as power spectral densities for one operational
flight of a fighter airplane. The frequency content, which is described
by the shape of the spectrum, may be useful in providing inputs for the
design of power control systems. Although the data presented are limited,
they indicate that for load factor the results presented for the opera-
tional flight considered are in general agreement with the results of more
complete data on three fighter airplanes.

The results indicate that the frequency content for the three con-
trol positions was similar and that the frequency content for the three
angular velocities was also similar when normalized by dividing by the
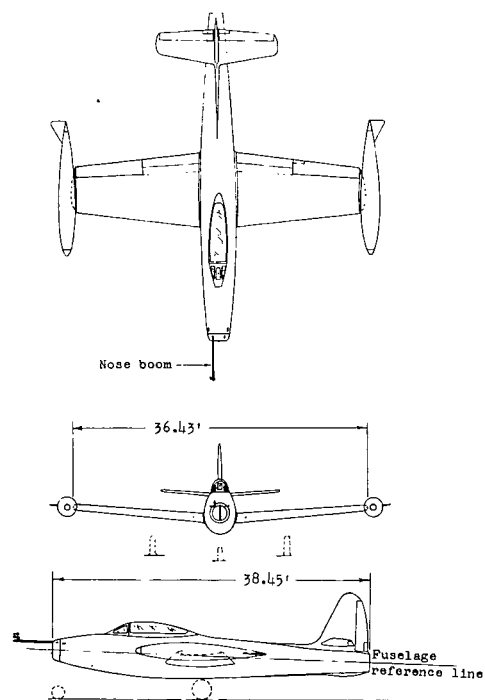mean-square value.

The spectrum of angular acceleration derived from the spectrum of
angular velocity was shown to be in good agreement with the results of
the spectrum obtained from direct measurements of angular acceleration.

███████

It was also shown that the use of the theoretical input-output relation-
ship to obtain the elevator spectrum from the normal-load-factor spectrum
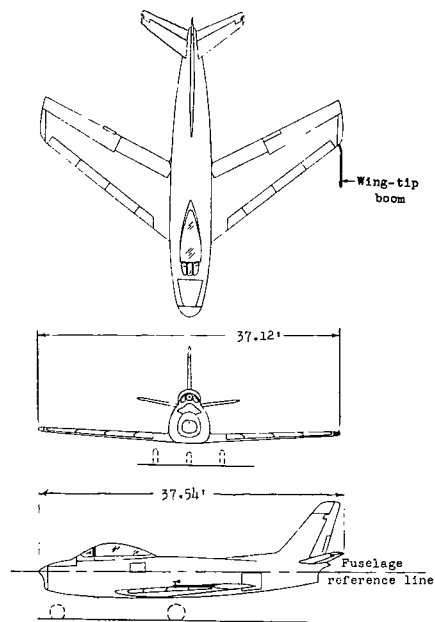produced satisfactory results.

Langley Aeronautical Laboratory,
    National Advisory Committee for Aeronautics,
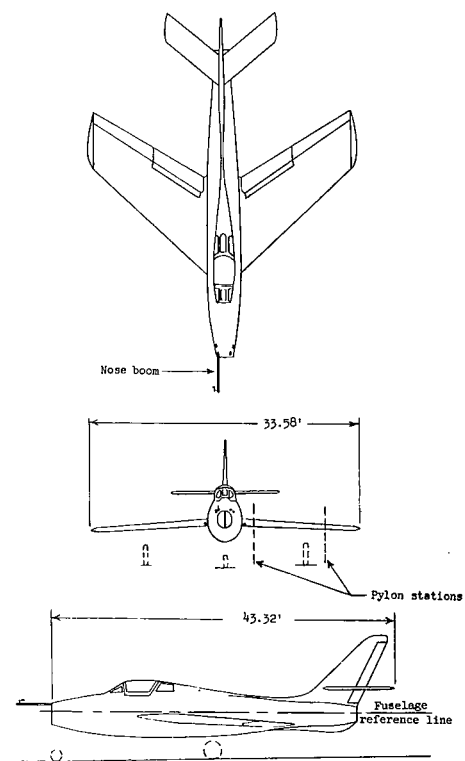   Langley Field, Va., April 26, 1957.

REFERENCES

1. Mayer, John P., Hamer, Harold A., and Huss, Carl R.: A Study of the
   Use of Controls and the Resulting Airplane Response During Service
   Training Operations of Four Jet Fighter Airplanes. NACA RM L53L28,
   1954.

2. Mayer, John P., and Hamer, Harold A.: A Study of Service-Imposed
   Maneuvers of Four Jet Fighter Airplanes in Relation to Their
   Handling Qualities and Calculated Dynamic Characteristics. NACA
   RM L55E19, 1955.

3. Mayer, John P., and Hamer, Harold A.: Applications of Power Spectral
   Analysis Methods to Maneuver Loads Obtained on Jet Fighter Airplanes
   During Service Operations. NACA RM L56J15, 1957.

4. Press, Harry, and Tukey, John W.: Power Spectral Methods of Analysis
   and Their Application to Problems in Airplane Dynamics. Vol. IV of
   AGARD Flight Test Manual, Pt. IV C, Enoch J. Durbin, ed., North
   Atlantic Treaty Organization, June 1956, pp. IVC:1-IVC:41.

Nose boom

Wing-tip boom

Nose boom

36.43'

37.12'

33.58'

Pylon stations

38.45'

Fuselage reference line

37.54'

Fuselage reference line

43.32'

Fuselage reference line

F-84G

F-86A

F-84F

Figure 1.- Three-view drawings of test airplanes.
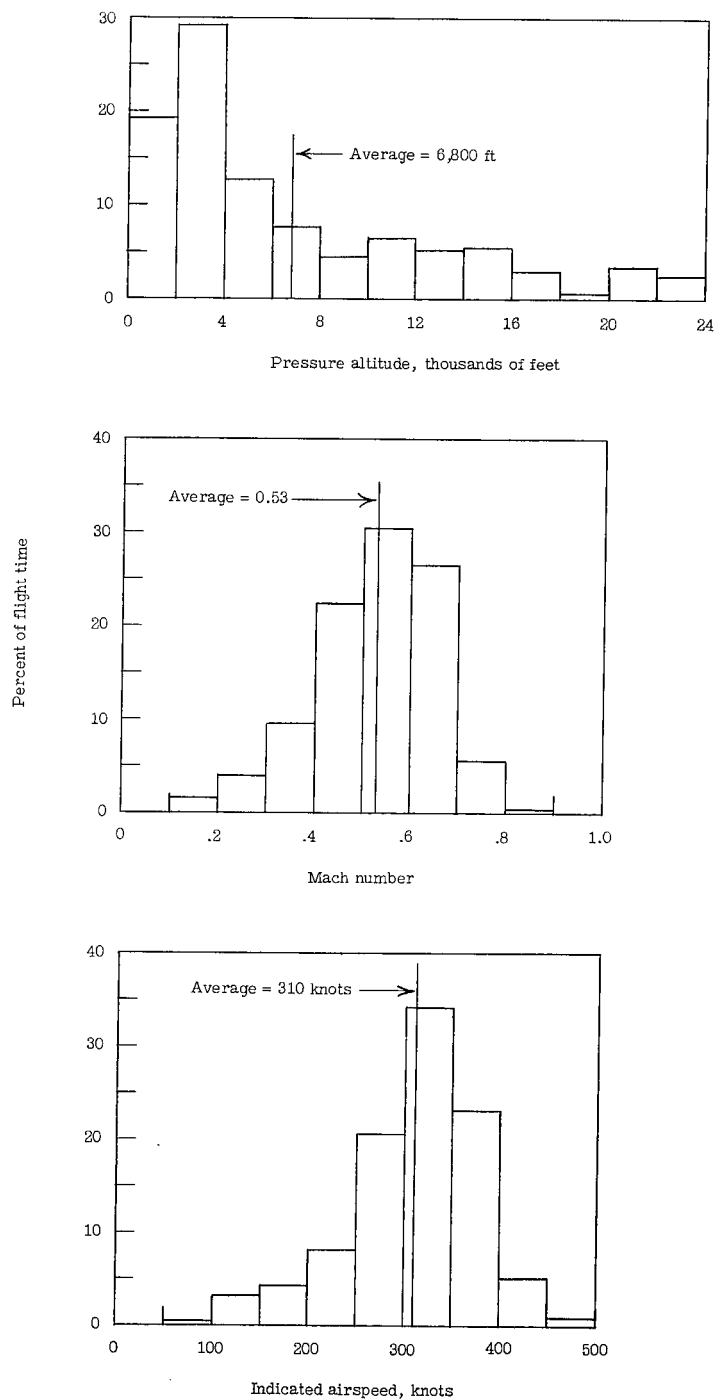
Figure 2.- Distribution of airspeed, Mach number, and altitude.
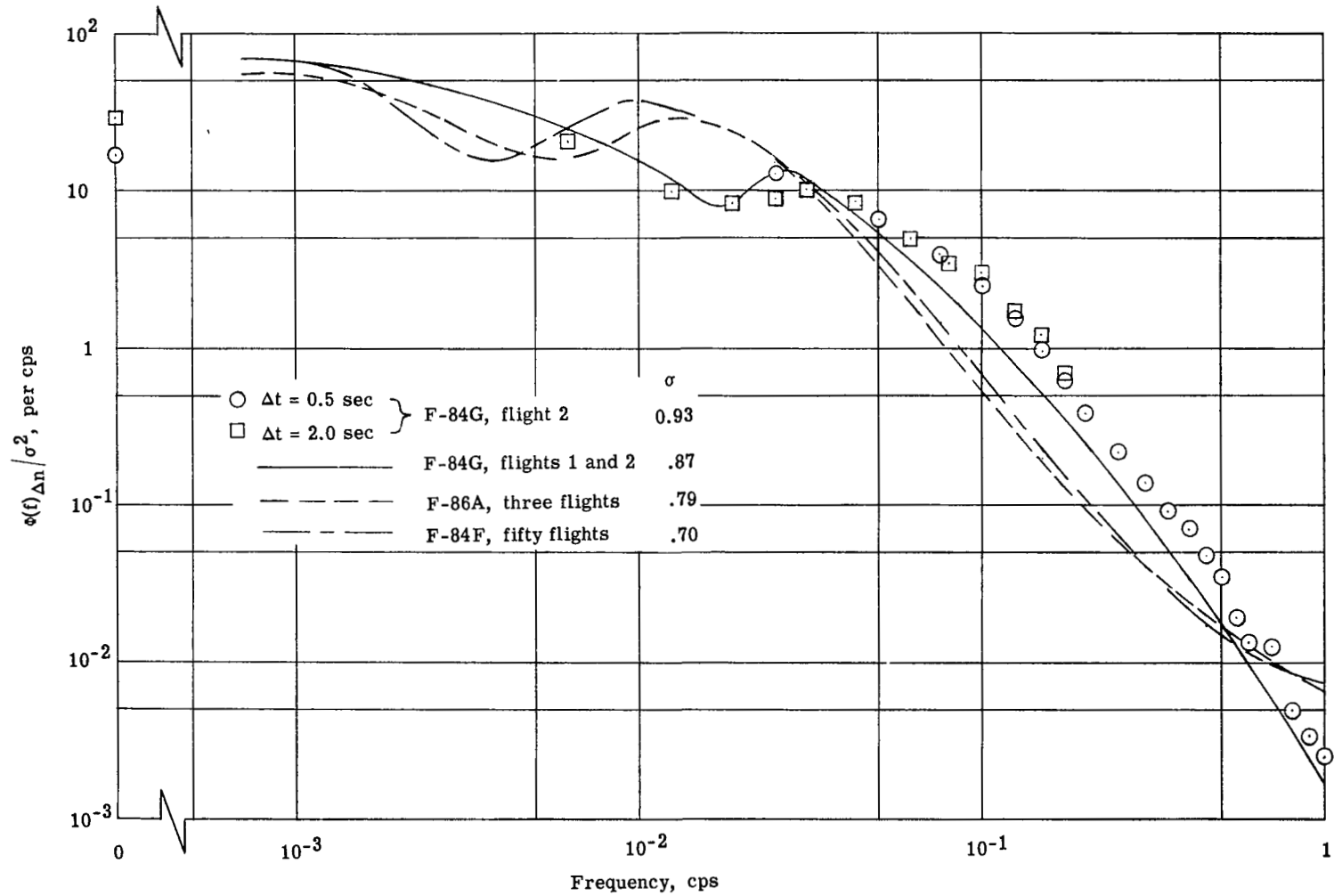Republic F-84G airplane.

10^2

10

1

10^{-1}

10^{-2}

10^{-3}

$\frac{\Phi(f)_{\Delta n}}{\sigma^2}$, per cps

		σ
◯ $\Delta t = 0.5$ sec	} F-84G, flight 2	0.93
☐ $\Delta t = 2.0$ sec		
———	F-84G, flights 1 and 2	.87
— — —	F-86A, three flights	.79
— · — · —	F-84F, fifty flights	.70

0 10^{-3} 10^{-2} 10^{-1} 1

Frequency, cps

Figure 3.- Power spectral densities of normal load factor.
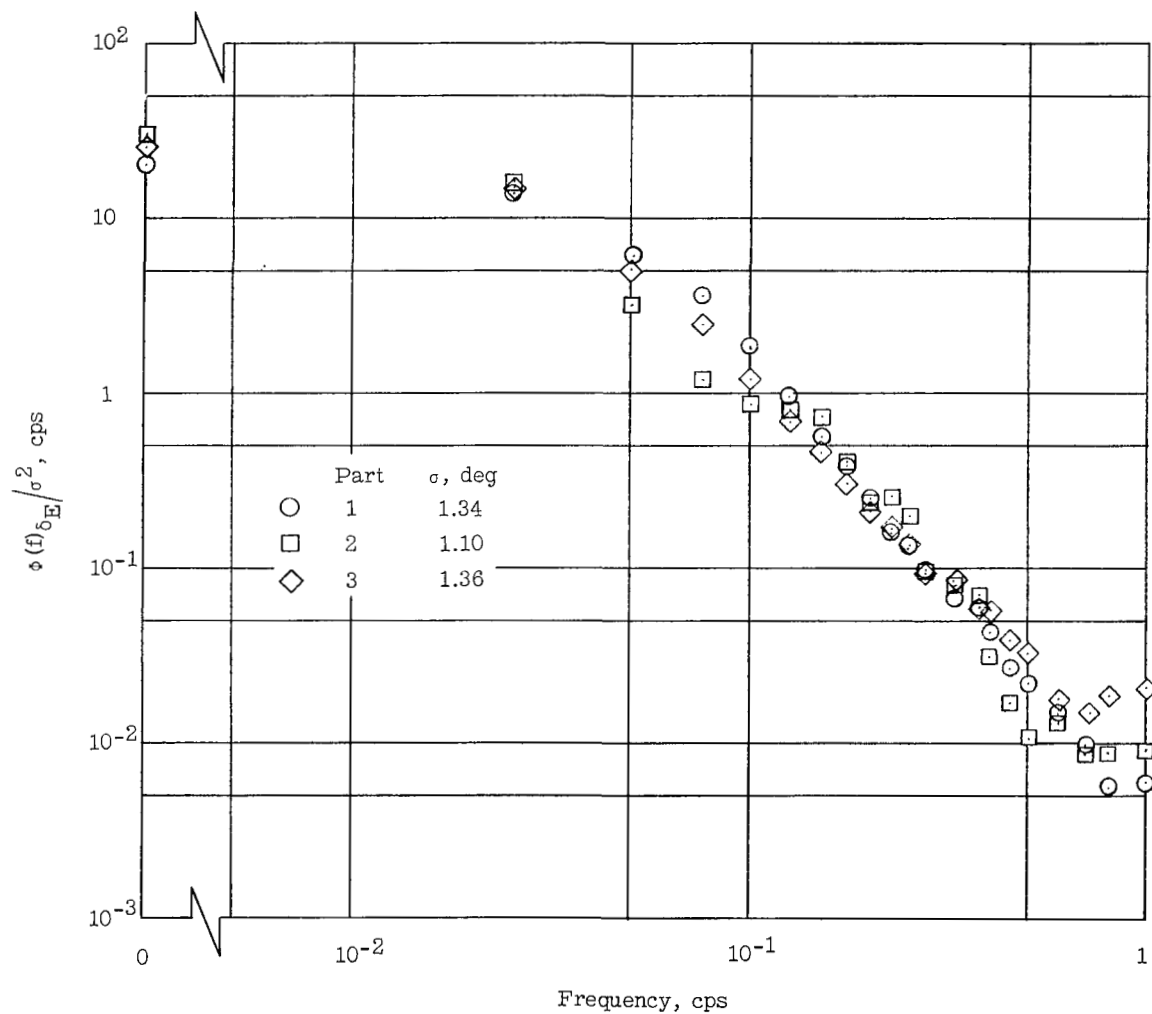
Figure 4.- Power spectral densities of elevator angle for three parts
of flight 2 of the Republic F-84G airplane.
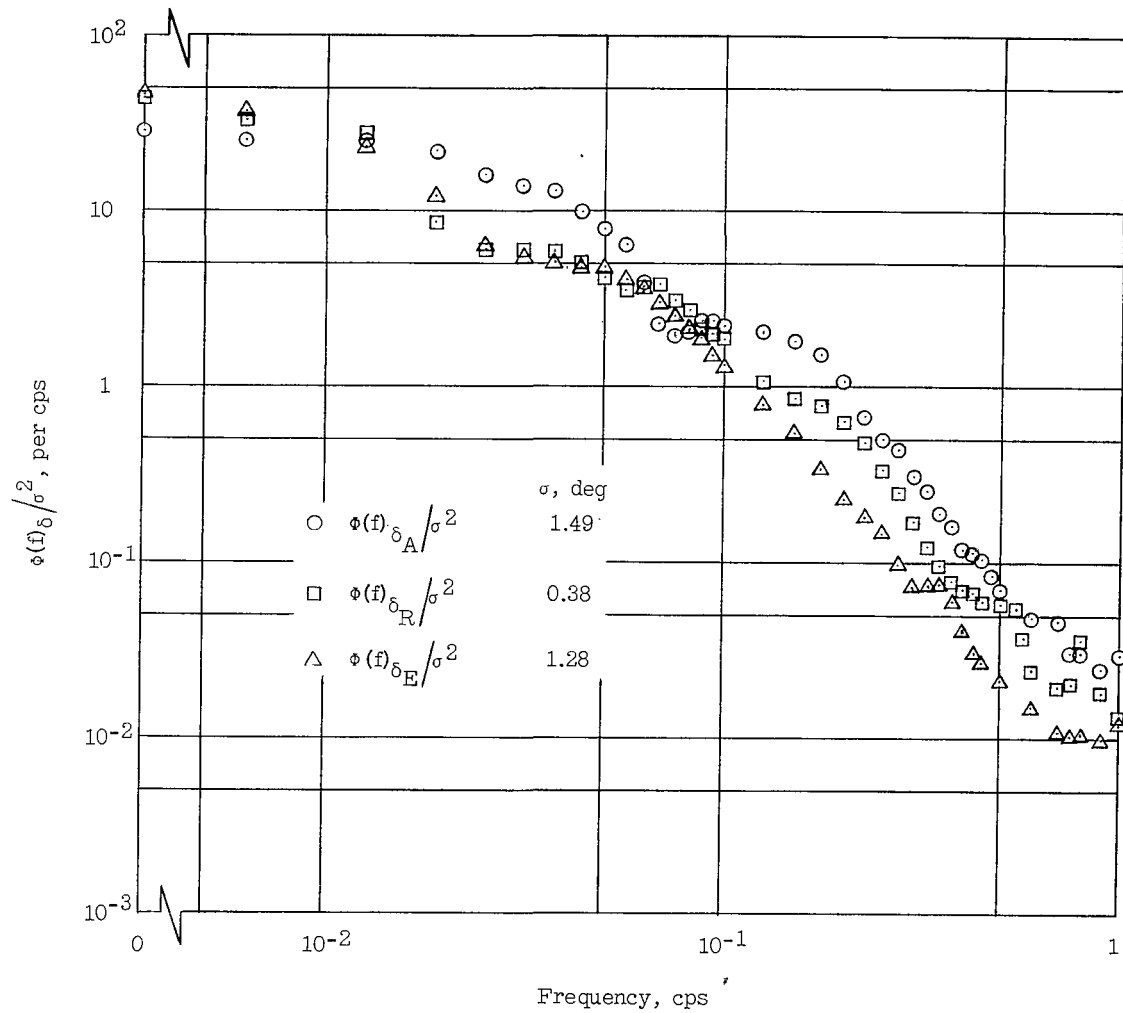
Figure 5.- Power spectral densities of control positions.   Republic F-84G
airplane, flight 2.
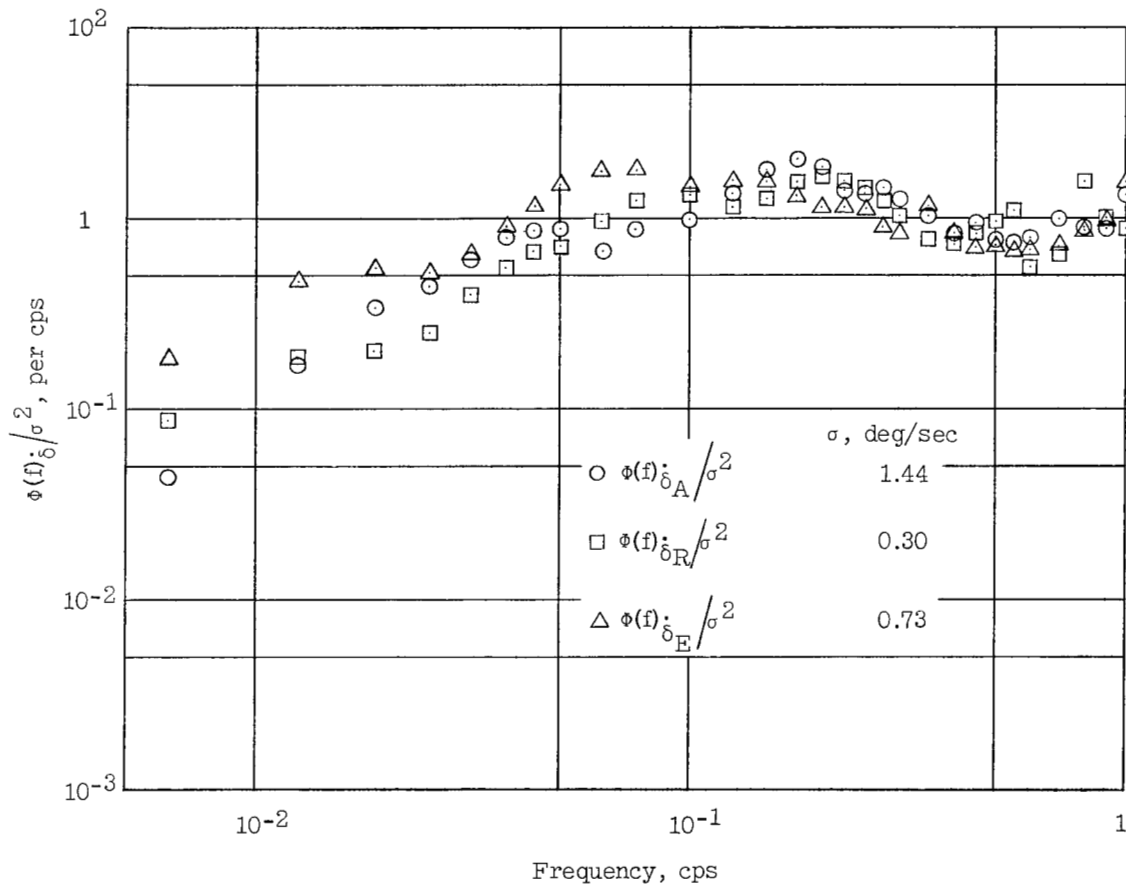
Figure 6.- Power spectral densities of control rates. Republic F-84G airplane, flight 2.
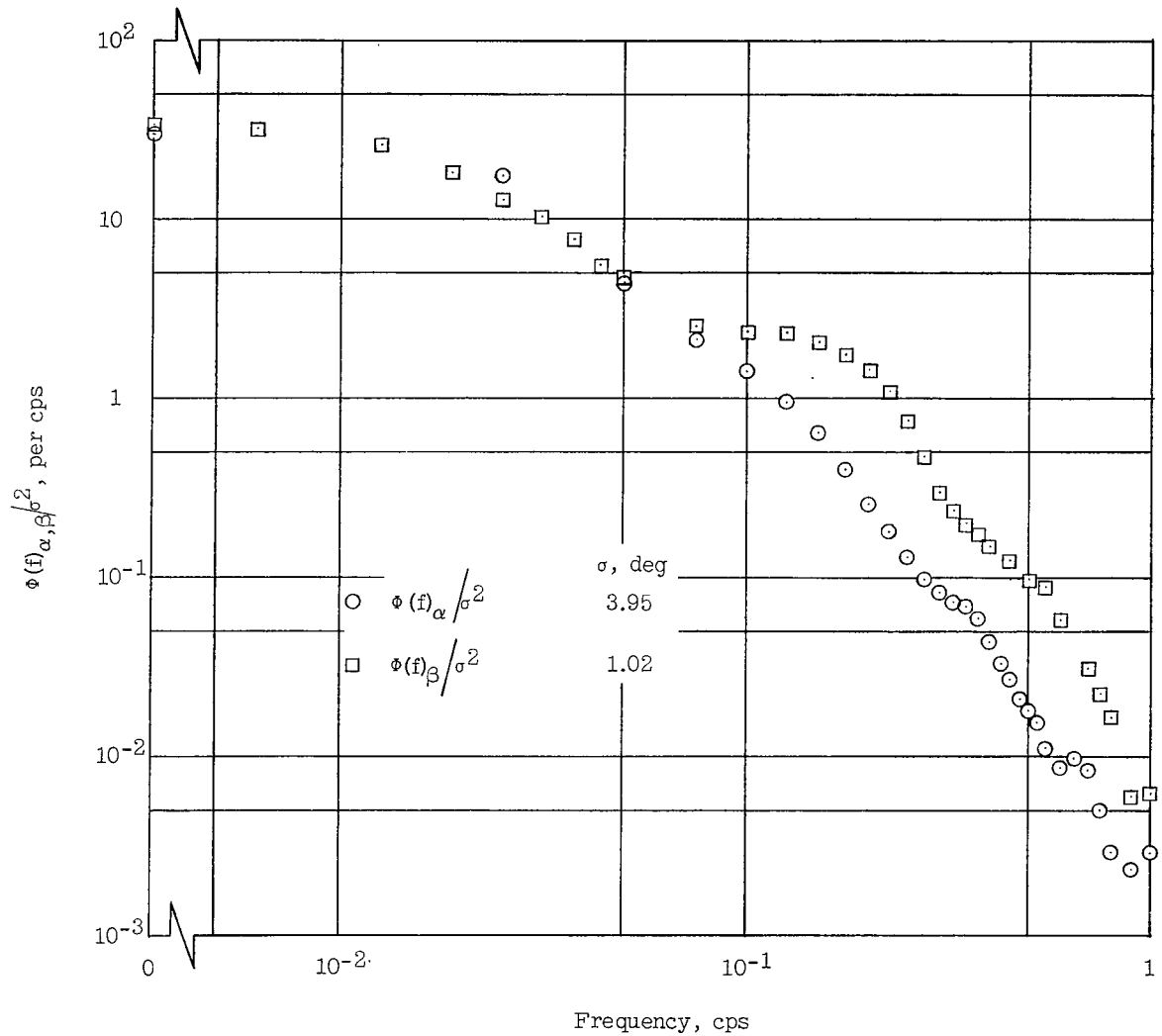
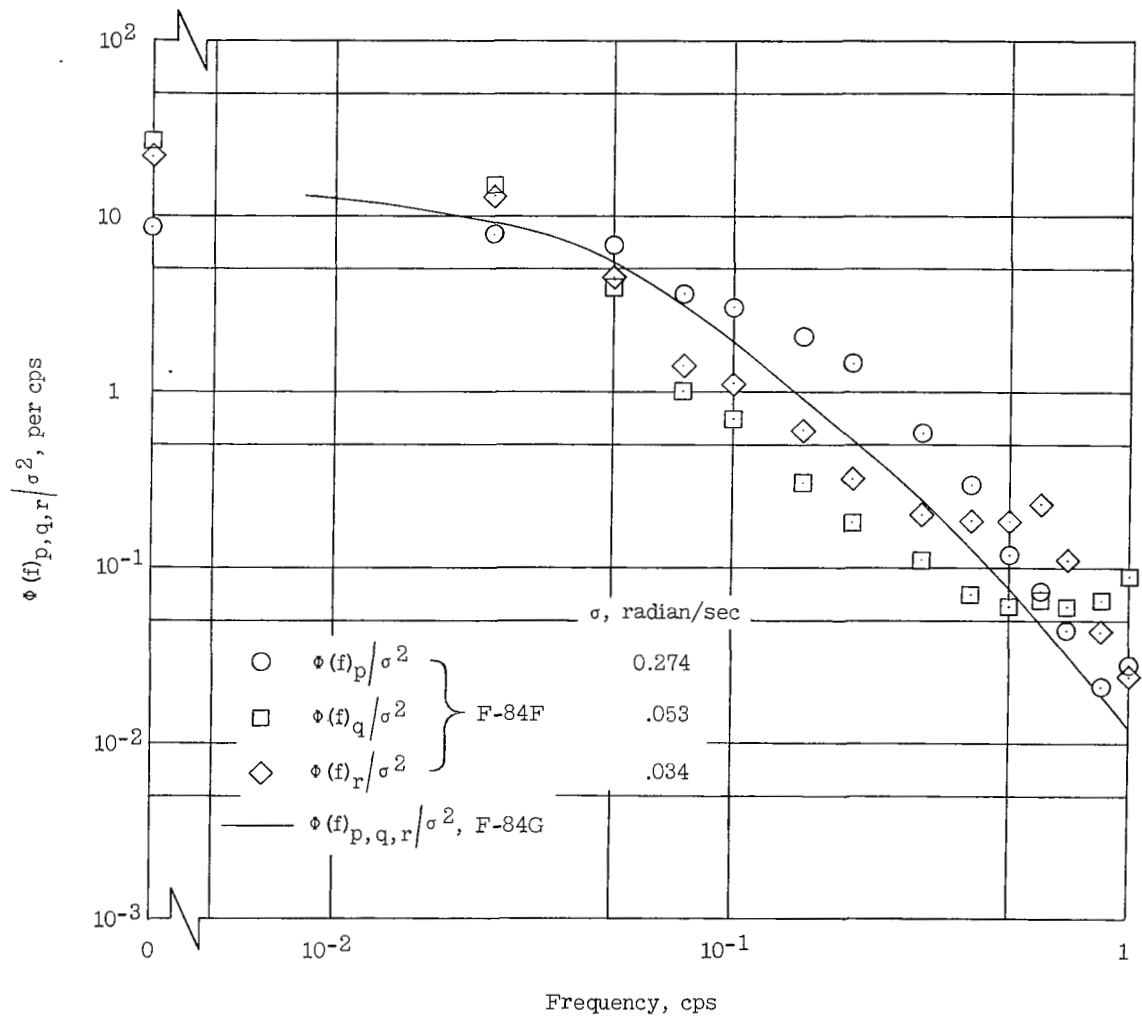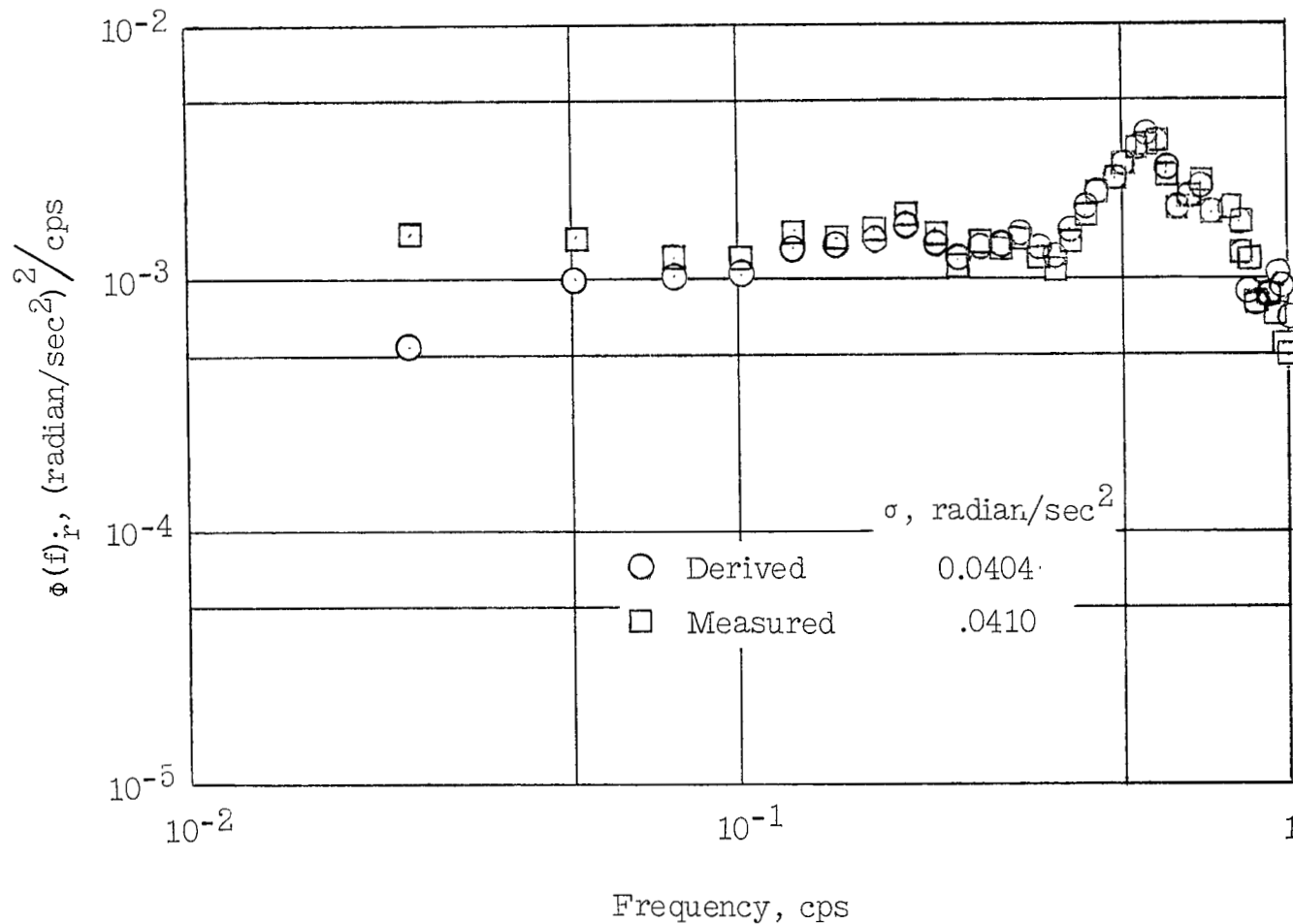Figure 7.- Power spectral densities of angle of attack and angle of side-slip. Republic F-84G airplane, flight 2.
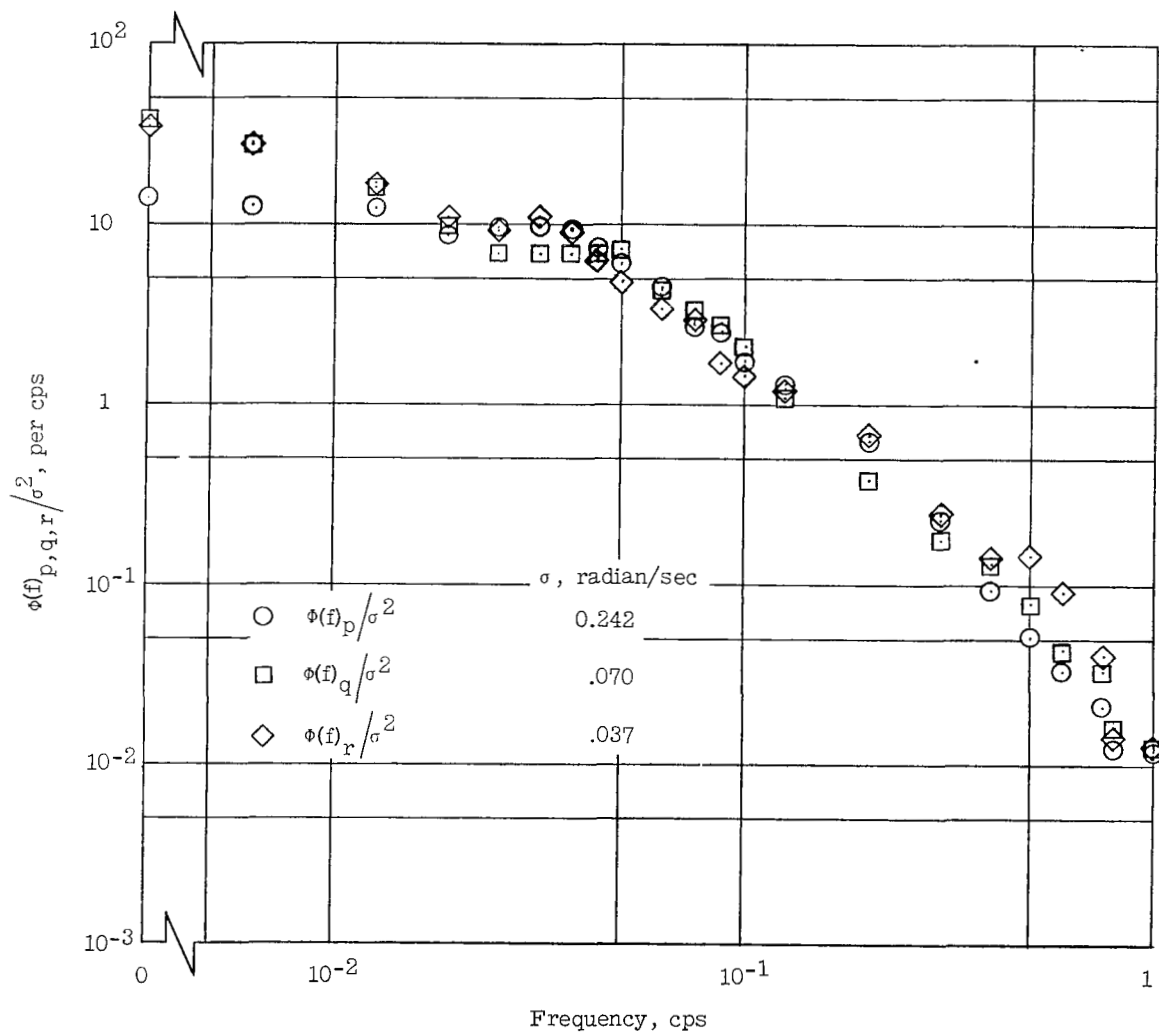
Figure 8.- Power spectral densities of angular velocities. Republic F-84G
airplane, flight 2.

Figure 9.- Power spectral densities of angular velocities for one flight
of the Republic F-84F airplane.
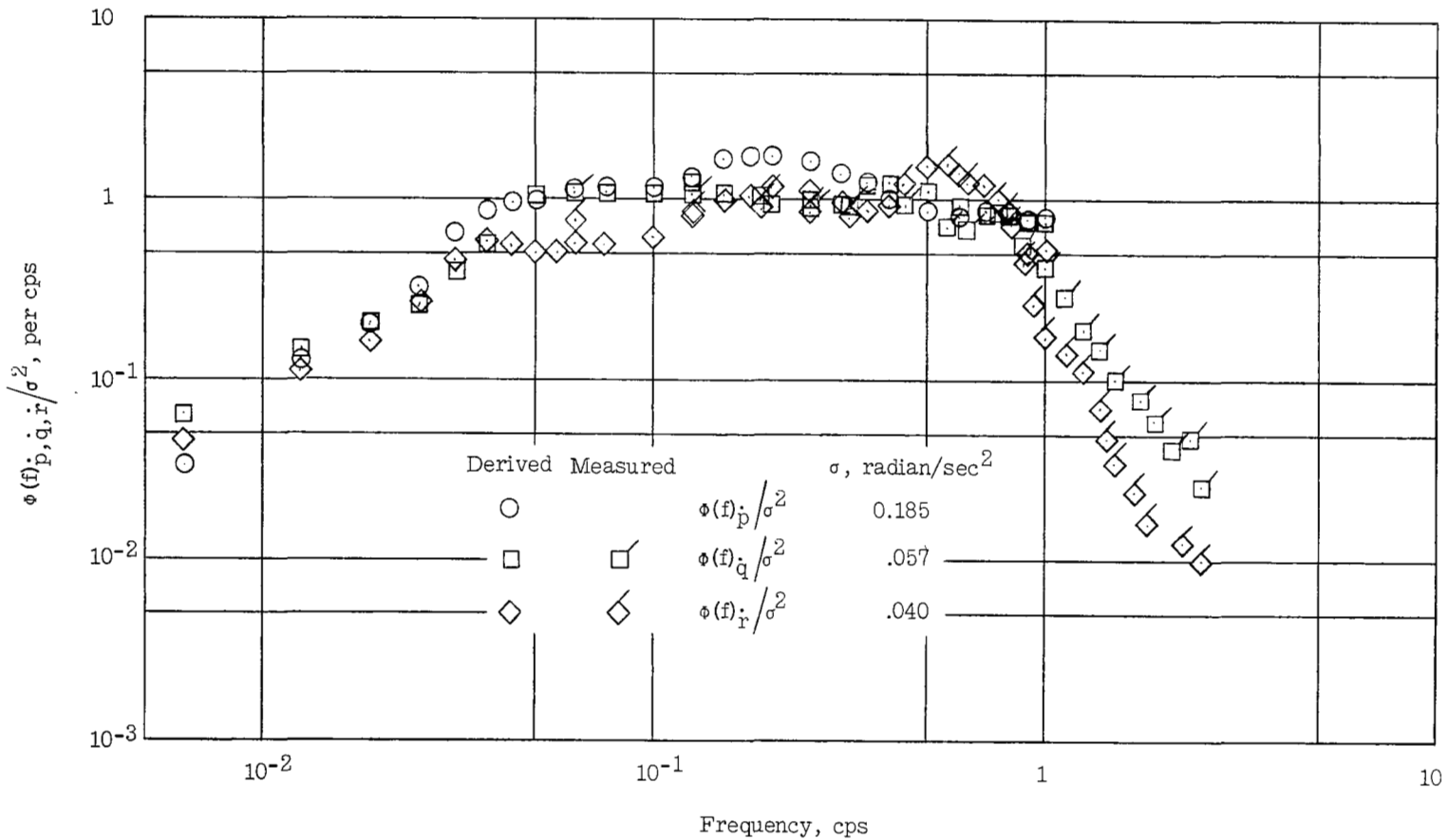
Figure 10.- Power spectral densities of angular accelerations. Republic F-84G airplane, flight 2.

Figure 11.- Comparison of measured and derived power spectral densities of yawing acceleration. Republic F-84G airplane, flight 2.
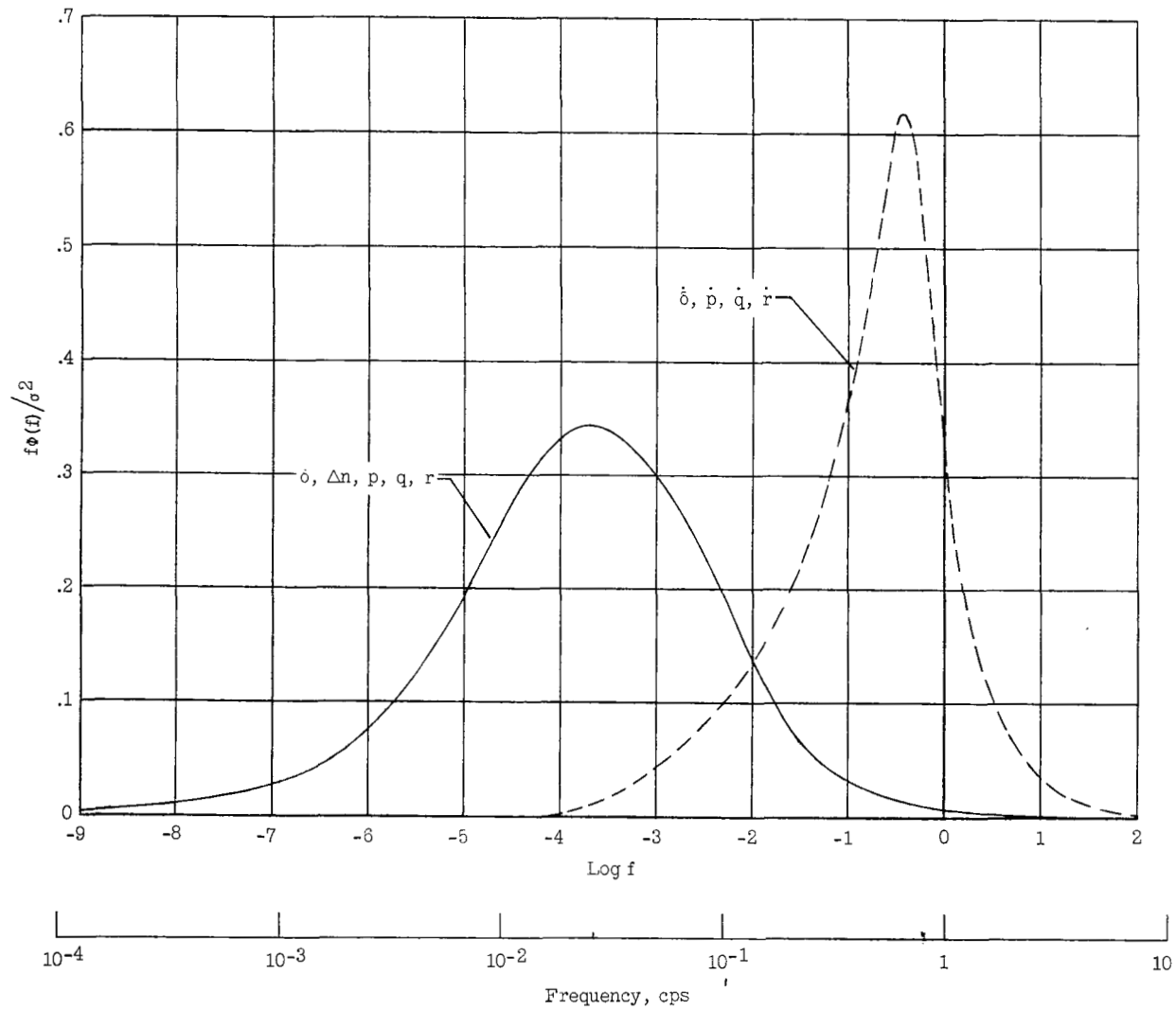
Figure 12.- Illustration of significant frequency ranges in control-input and airplane-response spectra.
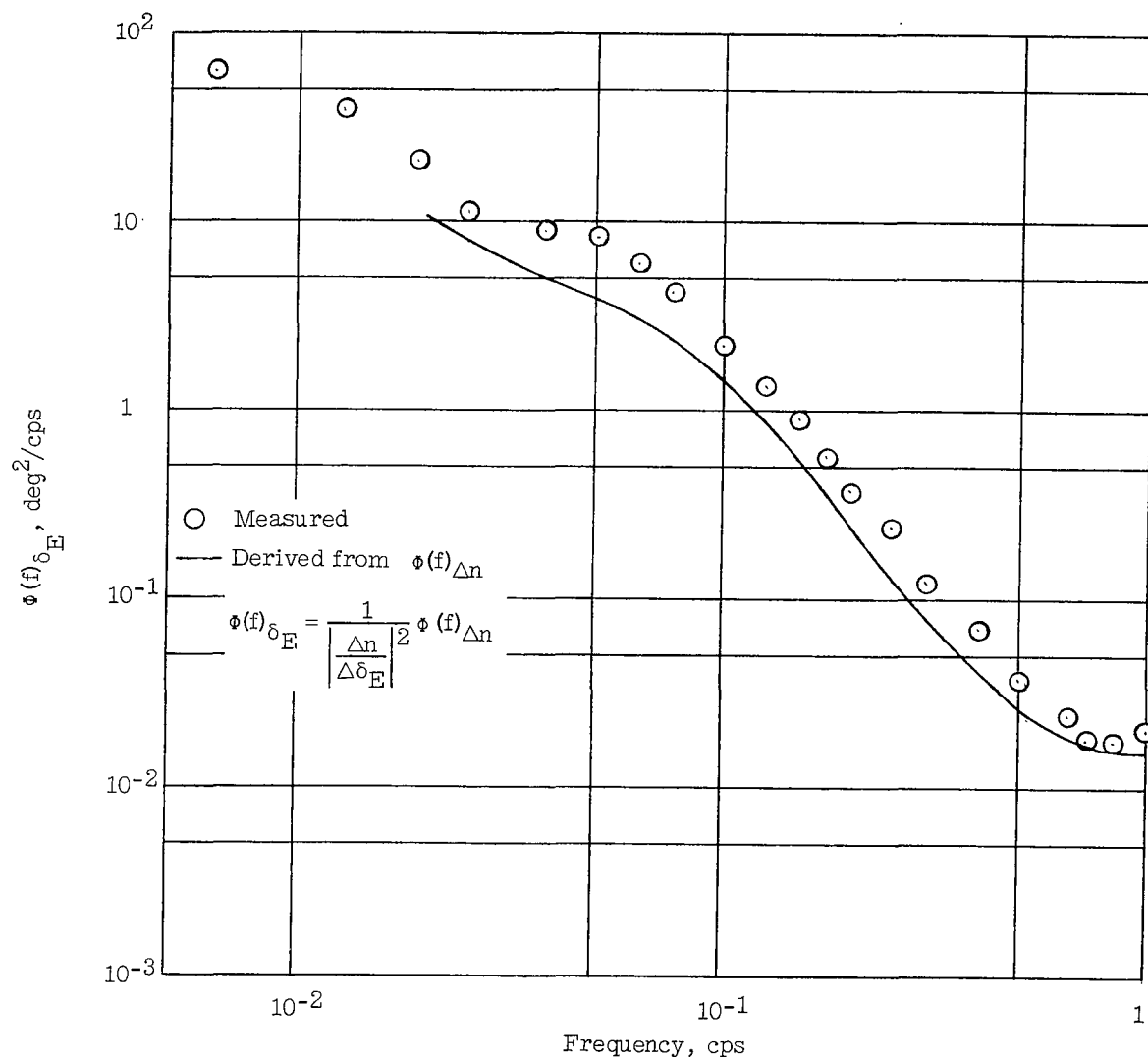
Figure 13.- Comparison of measured and derived power spectra of elevator angle. Republic F-84G airplane.